

# Cluster Assisted Water Dissociation Mechanism in MOF-74 and Controlling it Using Helium

S. Zuluaga,<sup>1</sup> E. M. A. Fuentes-Fernandez,<sup>2</sup> K. Tan,<sup>2</sup> J. Li,<sup>3</sup> I. J. Chabal,<sup>2</sup> and T. Thonhauser<sup>1,\*</sup>

<sup>1</sup>*Department of Physics, Wake Forest University, Winston-Salem, North Carolina 27109, USA*

<sup>2</sup>*Department of Materials Science and Engineering, University of Texas at Dallas, Richardson, Texas 75080, USA*

<sup>3</sup>*Department of Chemistry and Chemical Biology, Rutgers University, Piscataway, New Jersey 08854, USA*

(Dated: October 29, 2018)

We show that the water dissociation reaction  $\text{H}_2\text{O} \rightarrow \text{OH}+\text{H}$  in the confined environment of MOF-74 channels can be precisely controlled by the addition of the noble gas He. Elucidating the entire reaction process with *ab initio* methods and infrared (IR) spectroscopy, we prove that the interaction between water molecules is critical to the formation of water clusters, which reduce the dissociation barrier by up to 37% and thus influence the reaction significantly. Our time-resolved IR measurements confirm that the formation of these clusters can be suppressed by introducing He gas, providing unprecedented control over water dissociation rates. Since the water dissociation reaction is the cause of the structural instability of MOF-74 in the presence of water, our finding of the reaction mechanism lays the groundwork for designing water stable versions of MOF-74 as well as understanding water related phenomena in MOFs in general.

## I. INTRODUCTION

Metal organic framework (MOF) materials in general—and MOF-74 [ $\mathcal{M}_2(\text{dobdc})$ ,  $\mathcal{M} = \text{Mg}^{2+}$ ,  $\text{Zn}^{2+}$ ,  $\text{Ni}^{2+}$ ,  $\text{Co}^{2+}$ , and  $\text{dobdc}=2,5$ -dihydroxybenzenedicarboxylic acid] with its high density of coordinatively unsaturated metal ions in particular—have shown promising properties for technologically critical applications such as gas storage and sequestration,<sup>1–5</sup> catalysis,<sup>6,7</sup> polymerization,<sup>8,9</sup> luminescence,<sup>10,11</sup> nonlinear optics,<sup>12</sup> magnetic networks,<sup>13</sup> targeted drug delivery,<sup>14</sup> multiferroics,<sup>15–17</sup> and sensing.<sup>18–22</sup> This versatility is the result of MOF’s simple nano-porous building-block nature and affinity towards small molecule adsorption. Unfortunately, despite its great potential, the practical use of MOF-74 in such applications is rather limited due to its low stability and reduction of gas uptake capacity in the presence of water vapor.<sup>23–27</sup>

The interaction mechanism of MOF-74 with water has long been a mystery, as no clear spectroscopic signature could be observed. The only hint that a reaction occurred was a decrease in small-molecule uptake and the loss of crystal structure of some MOF-74 members after exposure to water.<sup>23–27</sup> Progress in the understanding of the interaction between water and MOF-74 came only recently through infrared (IR) absorption spectroscopy, which identified the fingerprint of a water dissociation reaction  $\text{H}_2\text{O} \rightarrow \text{OH}+\text{H}$  at temperatures above 150 °C.<sup>28,29</sup> This fingerprint consists of a clear peak in the IR spectrum at 970  $\text{cm}^{-1}$ , which by fortuitous coincidence falls into the phonon gap of the MOF-74 spectrum, when exposing e.g. Zn-MOF-74 to  $\text{D}_2\text{O}$ , see Fig. 1. The corresponding peak for the same reaction with  $\text{H}_2\text{O}$  is at 1316  $\text{cm}^{-1}$  and thus outside the phonon gap, where it strongly coupling with other MOF phonon modes and becomes impossible to detect.

The  $\text{H}_2\text{O} \rightarrow \text{OH}+\text{H}$  reaction in MOF-74 has been linked to its  $\text{CO}_2$  uptake reduction and structural insta-

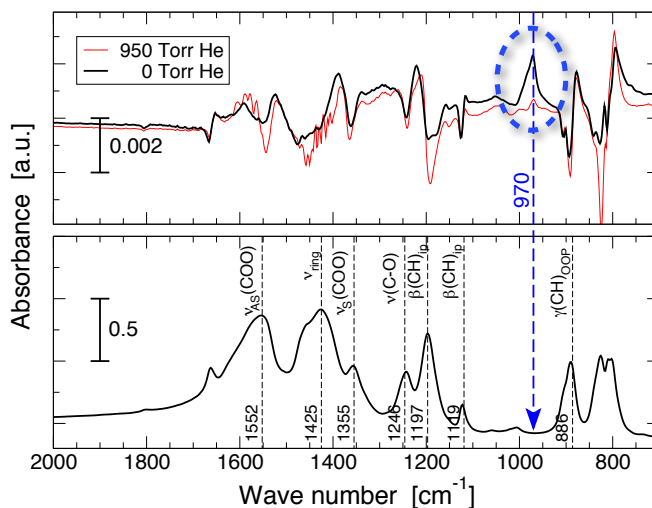


FIG. 1. (bottom) IR absorption spectra of activated Zn-MOF-74 referenced to the KBr pellet. (top) IR absorption of Zn-MOF-74 after being exposed to 8 Torr of  $\text{D}_2\text{O}$  for 60 min. at 180 °C, with and without the presence of He; both spectra are referenced to the activated sample in the bottom panel. The fingerprint of the water dissociation reaction is clearly visible as a large peak appearing at 970  $\text{cm}^{-1}$ , falling into the phonon gap of the activated sample. Repeating the experiment with 950 Torr of He added shows that this fingerprint disappears again.

bility in the presence of water<sup>28,30</sup> and the exact relationship between them has just recently been discovered.<sup>31</sup> Therefore, if we are able to suppress the water dissociation reaction, we are in a position to control the reduction in gas uptake capacity and maintain the crystal structure under humid conditions. In this work, we present our study on how the  $\text{H}_2\text{O} \rightarrow \text{OH}+\text{H}$  reaction takes place inside MOF-74 and use our findings to design a simple but elegant experiment that shows a means to control the reaction. With this proof-of-principle approach, our work

lays the foundation for a concise understanding of the water dissociation mechanism in MOF-74, opening the door for the rational design of water stable MOF-74. It is likely that a suppression of the dissociation reaction can also be achieved via co-adsorption of other molecules alongside water,<sup>32</sup> but we focus on only water here since it binds strongest amongst many small molecules.<sup>33</sup> For our study we use Zn-MOF-74, as it has the highest catalytic activity amongst the isostructural MOF-74 family for water dissociation.<sup>28</sup> Note that the catalytic activity linearly increases as the size of the metal decreases,<sup>31</sup> and we find that the catalytic activity towards the  $\text{H}_2\text{O} \rightarrow \text{OH}+\text{H}$  reaction is greatest in Zn-MOF-74, followed by Mg-, Ni-, and Co-MOF-74, in that order. We will show that this behavior has its roots in the fact that—in order for the  $\text{H}_2\text{O} \rightarrow \text{OH}+\text{H}$  reaction to take place—the water clusters need to interact with the metal center and the linker at the same time. As the metal center becomes smaller, it pulls the water molecules closer to the corner of the MOF and thus enhances also the interaction of the water with the linker. Note that for simplicity we may use the word “water,” but actually refer to “heavy water,” i.e.  $\text{D}_2\text{O}$ .

## II. BARRIER TO WATER DISSOCIATION

We begin by using *ab initio* simulations to analyze the  $\text{H}_2\text{O} \rightarrow \text{OH}+\text{H}$  reaction at the metal centers of Zn-MOF-74 and, in particular, how other water molecules affect it. For this purpose, we considered  $n = 1, 2, 3, 4,$  and  $5$  water molecules near one metal site, which form small water clusters. The energy profile along the  $\text{H}_2\text{O} \rightarrow \text{OH}+\text{H}$  reaction pathway and its thermodynamics for the various clusters are given in Fig. 2; actual values for activation barriers ( $E_B$ ) are collected in Table I. For a single water molecule cluster ( $n = 1$ ), we find a reaction barrier of 1.09 eV. The  $\text{H}_2\text{O} \rightarrow \text{OH}+\text{H}$  reaction path corresponds to Fig. 3, where the adsorbed water transfers one hydrogen to the nearest oxygen of the linker, as discussed in detail elsewhere.<sup>28</sup> The stable states of these clusters before the dissociation reaction are depicted in the upper row of Fig. 3; the lower row shows their counter parts, once the dissociation reaction has taken place. Note that for large enough clusters, the clusters start interacting with one additional water molecule at the nearby metal site and we have not included that molecule in our count of  $n$ , i.e. there are  $n + 1$  water molecules in each figure. The water molecules in the clusters interact via H bonds, similar to their behavior on the surface of metals and other systems.<sup>34–40</sup>

Looking at the barriers for water clusters with  $n = 1$  to 3, we see that they only decrease slightly, see Table I and Fig. 2. In these cases, the additional water molecules act as catalysts and the reaction proceeds just like in the case of a single water molecule—i.e. the water molecule at the metal center donates its H to the oxygen of the linker, see Fig. 3. Other groups have suggested a similar effect on metal oxide surfaces, called water catalyzed

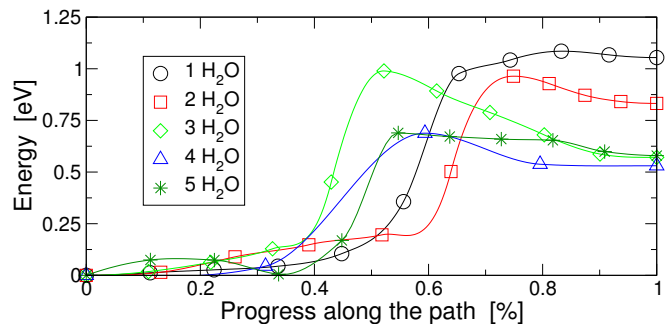


FIG. 2. Relative energy [eV] along the water dissociation reaction  $n \text{H}_2\text{O} \rightarrow \text{OH}+\text{H}+(n-1) \text{H}_2\text{O}$  in Zn-MOF-74 for  $n = 1$  to 5. The maxima for each line, i.e. the activation barrier, are tabulated in Table I.

TABLE I. Activation barrier  $E_B$  [eV] for the water dissociation reaction  $n \text{H}_2\text{O} \rightarrow \text{OH}+\text{H}+(n-1) \text{H}_2\text{O}$  at one metal center in Zn-MOF-74. Figure 2 shows the energy along the entire reaction pathway. We also list formation energies per water molecule  $E_F$  [eV] for all clusters.

| $n$   | 1     | 2     | 3     | 4     | 5     |
|-------|-------|-------|-------|-------|-------|
| $E_B$ | 1.09  | 0.96  | 0.99  | 0.69  | 0.69  |
| $E_F$ | -0.57 | -0.57 | -0.61 | -0.62 | -0.62 |

dissociation induced by collective interaction,<sup>41–44</sup> where the interactions among water molecules play an important role, responsible for a change in the structure and proton-transfer dynamics. However, in our case the interaction among water molecules plays an additional role, as we show next: for  $n > 3$  we observe a dramatic 37% reduction in the activation barrier, see Table I and Fig. 2. This surprising and unexpected finding is the result of the water dissociation now proceeding through a completely different pathway. For  $n=4$  and 5 the geometry of the cluster allows for one of the water molecules to position above the linker, establishing a H bond with the O atom of the linker. This geometry opens up a much more favorable pathway. For example, Fig. 4 shows the  $\text{H}_2\text{O} \rightarrow \text{OH}+\text{H}$  reaction path for the  $n = 4$  case: Water molecule **A** donates one H to molecule **B**, which, at the same time donates one H to the oxygen at the linker—an animation of this reaction is available in the supplementary materials. We have also investigated the case of  $n = 5$ , in which the reaction proceeds similarly to the  $n = 4$  case. Note that this is vastly different from the cases of  $n = 1$  to 3, where the H being donated to the linker comes from the water adsorbed at the nearby metal center.

The key to this drastic lowering of the energy barrier for  $n > 3$  is the water molecule above the linker. The  $\text{H}_2\text{O} \rightarrow \text{OH}+\text{H}$  reaction can proceed through this low energy-barrier path only if one of the water molecules in the cluster has a strong interaction with the O of the linker. In other words, one water molecule needs to be close to the O of the linker. The top row of Fig. 3

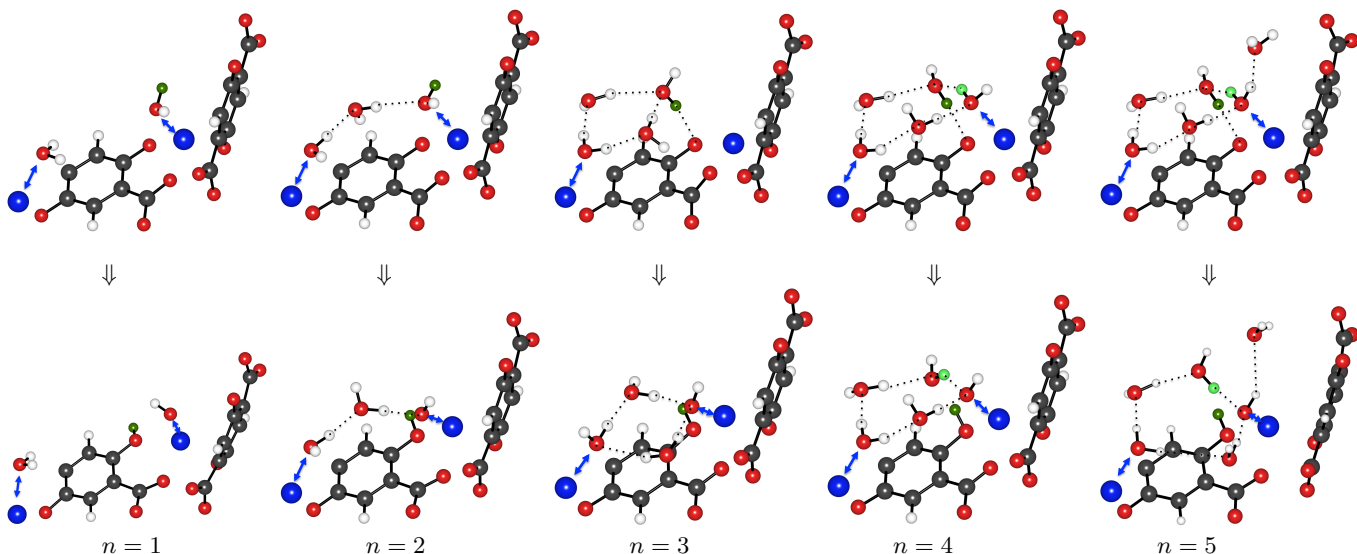


FIG. 3. Water cluster geometries for  $n = 1, 2, 3, 4,$  and  $5$  before (upper row) and after (lower row) the  $\text{H}_2\text{O} \rightarrow \text{OH} + \text{H}$  reaction takes place. Red, white, black, and blue spheres represent O, H, C, and Zn atoms. Blue arrows indicate bonds between the water molecules and metal centers, while dashed black lines indicate H–O bonds. H atoms that are transferred are colored in green. The figure only shows a small portion of MOF-74.

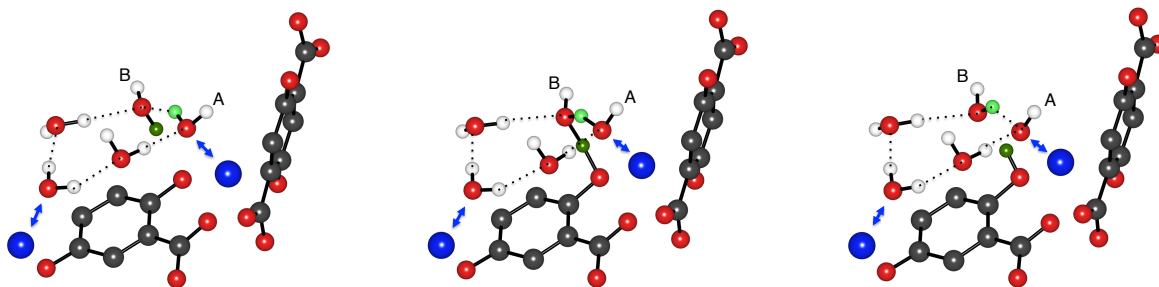


FIG. 4. Initial, transition, and final state of the water dissociation pathway corresponding to  $n = 4$ . The reaction takes place through the following low-energy barrier path: **A** donates one H to **B**, which—at the same time—donates one H to the oxygen of the linker. Red, white, black, and blue spheres represent O, H, C, and Zn atoms; the hydrogens being transferred are shown in green. See the corresponding animation in the supplementary materials. The figure only shows a small portion of MOF-74.

shows the configuration of the water molecules before the  $\text{H}_2\text{O} \rightarrow \text{OH} + \text{H}$  reaction takes place for  $n = 1, 2, 4,$  and  $5$ . For  $n = 4$  and  $5$ , we find that one of the water molecules is able to position itself above the linker and establish an H bond with the O of the linker, while for  $n = 1$  and  $2$  this is not possible. For comparison, in the  $n = 1$  case the water molecule adsorbed on the metal center is located  $3.64 \text{ \AA}$  away from the O of the linker, whereas for the  $n = 4$  case the water molecule is located only  $1.94 \text{ \AA}$  away. In Fig. 5 we analyze the role of this special water molecule near the O of the linker further. This figure shows the charge density redistribution upon adsorption of the water molecule **B**. We find significant charge accumulation (marked as red  $\times$  marks) between molecules **A** and **B**, and between molecule **B** and the linker. These strong bonds are responsible for the short distance between **A** and **B** ( $1.90 \text{ \AA}$ ) and between **B** and the O of the linker ( $1.94 \text{ \AA}$ ), allowing for the significantly reduced reaction barrier. Now also the function of the

other water molecules in the clusters for  $n = 4$  and  $5$  becomes apparent—the remaining water molecules forming the clusters serve to restrain **B** in its particular geometry above the O of the linker, making the close interaction with the linker and the reduced energy barrier possible.

Note that, even though for  $n = 3$  one water molecule is close to the O of the linker (see Fig. 3), the energy barrier for the reaction is still  $0.99 \text{ eV}$  (see Table I). The reason why the barrier is not reduced in this particular case is that, once the  $\text{H}_2\text{O}$  molecule loses its H, the remaining OH has to travel a long distance to the metal center in order to find a stable state.

Before we move on to the experimental verification of our discovered water dissociation mechanism, we would like to comment on two aspects. First, water dissociation in MOF-74 takes place at temperatures above  $150 \text{ }^\circ\text{C}$ .<sup>28</sup> Water clusters of such size as we are considering here may not be stable at such temperatures in their gas phase. However, the clusters inside MOF-74 are stabi-

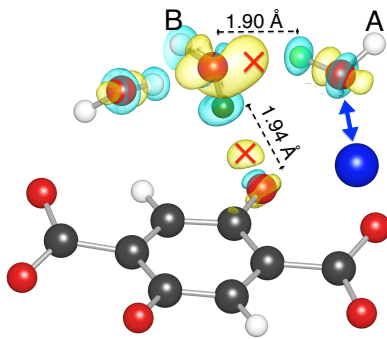


FIG. 5. Charge density redistribution upon adsorption of water molecule **B** for  $n = 4$ . Yellow denotes charge accumulation, while blue denotes charge depletion; the iso level is  $\pm 0.003 e/\text{\AA}^3$ . The red  $\times$  marks strong bonds between **A** and **B** and between **B** and the linker. For clarity, some water molecules and other elements of the system are not shown in this figure. Color coding as in Fig. 3.

lized through interaction with the linker. To quantify this aspect, we have calculated the formation energies per water molecule  $E_F$  for all clusters, reported in Table I. The numbers for all clusters inside MOF-74 ( $\sim -0.6$  eV) indicate a significantly higher stability than the corresponding number of  $-0.32$  eV for their gas-phase equivalents.<sup>39</sup> Second, due to the nature of transition-state search algorithms, the energy barriers reported in this work are an upper limit. There is a large number of stable initial and final configurations for water clusters that give rise to numerous possible reaction pathways. While we have modeled approximately 50 reactions, we only report the paths with the lowest energy barriers. For  $n > 5$  there may be other geometries that exhibit yet a lower energy barrier for the  $\text{H}_2\text{O} \rightarrow \text{OH}+\text{H}$  reaction. These paths may even have energy barriers closer to the splitting of water in other systems, where the energy barriers are as low as  $\sim 0.1$  eV.<sup>45–48</sup> However, a comprehensive *ab initio* sampling of larger clusters is prohibitively expensive. But, our main goal is not to find such paths or ways to dissociate water in MOF-74 in the most efficient manner. On the contrary, our goal is to understand the underlying mechanism and use this knowledge to avoid the  $\text{H}_2\text{O} \rightarrow \text{OH}+\text{H}$  reaction inside MOF-74. If we are able to do so, we would be able to avoid the poisoning of the metal centers (going hand-in-hand with a decrease of the small-molecule uptake capacity)<sup>28</sup> and the degradation of the crystal structure of the MOF-74 in the presence of water.<sup>30,31</sup> Our results suggest a way to accomplish exactly this goal: If we avoid the clustering of water molecules around the metal centers, we increase the energy barrier for the  $\text{H}_2\text{O} \rightarrow \text{OH}+\text{H}$  reaction from 0.69 eV (or lower) up to 1.09 eV, and the reaction will not take place at the temperatures at which MOF-74 is stable, i.e. between 0 and 300 °C. In the next section we show a way of achieving this.

### III. CONTROLLING WATER DISSOCIATION USING HE

Based on our theoretical results, we hypothesize that, if we are able to prevent the formation of these water clusters on the walls of MOF-74, we will be able to control and even suppress the water dissociation reaction, with important effects on the MOF’s stability and small-molecule uptake capacity. To test our hypothesis, we have designed an experiment where we control the formation of water clusters by introducing a non-reactive agent into the MOF-74 channel, such as He. More specifically, in addition to 8 Torr of  $\text{D}_2\text{O}$  we now introduce also 500 and 950 Torr of He into the activated Zn-MOF-74 at 180 °C, see the experimental details section for further details. The role of these non-interacting He atoms is to get in-between the water molecules, decreasing their interaction, preventing hydrogen bonds, and thus hindering the formation of clusters. At the same time, the partial pressure of He provides an effective means of controlling the number of He atoms in each nano pore and thus the degree of water cluster formation. This directly affects the reaction barrier for the dissociation reaction and allows us to control the amount of water dissociated.

For reasons explained in the introduction, our experiments are performed with  $\text{D}_2\text{O}$  instead of  $\text{H}_2\text{O}$ . The  $\text{D}_2\text{O} \rightarrow \text{OD}+\text{D}$  reaction has a characteristic fingerprint in form of a clear peak in the IR spectrum at  $970 \text{ cm}^{-1}$  (see Fig. 1), the integrated area of which provides a quantitative measure of how much water has dissociated. Our experiment now proceeds to record the integrated area of this peak (normalized to 1) as a function of time for the three different He partial pressures; results are plotted in Fig. 6. As can be seen, the integrated area for the sample without He (0 Torr He) grows and saturates as the water molecules on the metal centers dissociate; the reaction reaches 63% of the saturation level in 39 minutes. However, as the He partial pressure increases, the water dissociation reaction is suppressed due to the higher activation barrier, as the water clusters are less likely to form. In turn, we find that for He partial pressures of 500 and 950 Torr, it takes 70 and 181 minutes to reach 63% of the saturation level, respectively, confirming our hypothesis and the cluster assisted water dissociation mechanism. As an example, the top panel of Fig. 1 shows the decrease of the peak at  $970 \text{ cm}^{-1}$  after 60 minutes when adding 950 Torr of He to the 8 Torr of  $\text{D}_2\text{O}$ .

We have also used non-reactive agents other than He to demonstrate the connection between cluster formation, reaction barrier, and water dissociation suppression. Our results indicate that, e.g. the introduction of Ar also reduces the rate at which the water dissociation reaction takes place. However, the effect is not as strong as for He. Using 950 Torr of Ar together with 8 Torr of  $\text{D}_2\text{O}$  at a temperature of 180 °C, we find that the  $\text{H}_2\text{O} \rightarrow \text{OH}+\text{H}$  reaction reaches 63% of the saturation level after 92 minutes. There is thus no particular requirement for the agent, besides being non-reactive, to

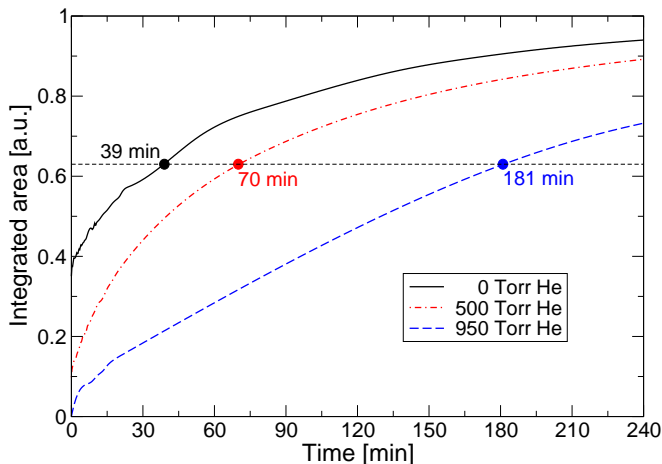


FIG. 6. Integrated area of the normalized peak at  $970\text{ cm}^{-1}$  from Fig. 1 as a function of time, giving a quantitative measure of the amount of water dissociated. All samples are exposed to 8 Torr of  $\text{D}_2\text{O}$  and a temperature of  $180\text{ }^\circ\text{C}$ . The black curve corresponds to the sample with no additional He, while the red, and blue curves correspond to the samples exposed to 500 and 950 Torr of He, respectively. The plot confirms that the water dissociation reaction is suppressed as higher partial pressures of He are introduced.

suppress the  $\text{H}_2\text{O} \rightarrow \text{OH}+\text{H}$  reaction. Nevertheless, He results were chosen here as the phenomena is stronger compare to Ar and others. We believe that He is a better reaction moderator because of its small size; it is fairly easy for He to penetrate in-between water molecules in the water clusters, suppressing their interaction and formation.

The partial pressures of He used in our experiments are large compared to the partial pressure of water. As such, it is not practical to use He to suppress the formation of water clusters. However, we see our experimental results not necessarily as a practical way in large applications to control the water dissociation, but rather as a proof-of-principle that such control is achievable. Furthermore, our experiments function also as crucial support for our *ab initio* results about how small water cluster formation aids the water dissociation. In future research, the design of a water stable MOF-74 has to begin by finding a way of suppressing the water cluster formation and the water dissociation reaction.

#### IV. SUMMARY

Our *ab initio* results show that the formation of water clusters on the walls of Zn-MOF-74 allows for an energetically much more favorable water dissociation path for the  $\text{H}_2\text{O} \rightarrow \text{OH}+\text{H}$  reaction. We then confirm via *in situ* IR spectroscopy that introducing He into the MOF channel to prevent the formation of such clusters is an effective way to suppress the water dissociation reaction. While we show results explicitly for He, it is quite likely

that other gases have the same effect. Since previous studies have indicated that the water dissociation reaction reduces MOF-74 gas uptake and crystal stability, we have thus found a proof-of-principle approach to control them. With this new insight, our results provide new opportunities for designing water stable MOF-74, focusing on the suppression of the water dissociation reaction which causes the problems.

## V. METHODS

### A. Computational Details

Our *ab initio* results were obtained at the density functional theory level, as implemented in QUANTUM ESPRESSO.<sup>49</sup> In order to correctly capture the crucial van der Waals interactions between the MOF and the water molecules, as well as between water molecules,<sup>39</sup> we used the truly non-local functional vdW-DF.<sup>50-53</sup> Nuclear quantum effects, which can play a noticeable role in the description of water and water dissociation,<sup>54</sup> were not taken into account due to the extreme computational cost. Ultrasoft pseudo potentials were used with cut-offs of 544 eV and 5440 eV for the wave functions and charge density, respectively. Due to the large dimensions of the unit cell, only the  $\Gamma$  point was sampled. Reaction barriers were found with a transition-state search algorithm, i.e. the climbing-image nudged-elastic band method,<sup>55,56</sup> using up to 11 images depending on the path. We started from the experimental rhombohedral structure of Zn-MOF-74 with 54 atoms in its primitive cell and space group  $R\bar{3}$ . The rhombohedral axes are  $a = b = c = 15.105\text{ \AA}$  and  $\alpha = \beta = \gamma = 117.78^\circ$ .<sup>57</sup> We optimized all atomic positions until the forces were less than  $2.6 \times 10^{-4}\text{ eV/\AA}$ .

### B. Experimental Details

Zn-MOF-74 powder ( $\sim 2\text{mg}$ ) was pressed onto a KBr pellet ( $\sim 1\text{cm}$  diameter, 1–2 mm thick). The sample was placed into a high-pressure high-temperature cell (product number P/N 5850c, Specac Ltd, UK) at the focal point compartment of an infrared spectrometer (Nicolet 6700, Thermo Scientific, US). The samples were activated under vacuum ( $< 20\text{ mTorr}$ ) at  $180\text{ }^\circ\text{C}$  for at least 4 hour. A mixture of He and  $\text{D}_2\text{O}$  was prepared in a compartment connected but separated from the main cell. Different ratios between He and  $\text{D}_2\text{O}$  were introduced into the main cell held at  $180\text{ }^\circ\text{C}$ : 950 Torr He/8 Torr  $\text{D}_2\text{O}$ ; 500 Torr He/8 Torr  $\text{D}_2\text{O}$ ; and 0 Torr He/8 Torr  $\text{D}_2\text{O}$ . The area under the peak at  $970\text{ cm}^{-1}$ , which is a quantitative measure of the amount of water dissociated in Zn-MOF-74, was measured as a function of time. Spectra were recorded until the reaction was saturated.

## ACKNOWLEDGEMENTS

This work was supported by the Department of Energy Grant No. DE-FG02-08ER46491. It further used

resources of the Oak Ridge Leadership Computing Facility at Oak Ridge National Laboratory, which is supported by the Office of Science of the Department of Energy under Contract DE-AC05-00OR22725.

- 
- \* thonhauser@wfu.edu
- <sup>1</sup> L. J. Murray, M. Dinca, and J. R. Long, *Chem. Soc. Rev.* **38**, 1294 (2009).
  - <sup>2</sup> J.-R. Li, Y. Ma, M. C. McCarthy, J. Sculley, J. Yu, H.-K. Jeong, P. B. Balbuena, and H.-C. Zhou, *Coord. Chem. Rev.* **255**, 1791 (2011).
  - <sup>3</sup> S. Qiu and G. Zhu, *Coord. Chem. Rev.* **253**, 2891 (2009).
  - <sup>4</sup> N. Nijem, H. Wu, P. Canepa, A. Marti, K. J. Balkus, T. Thonhauser, J. Li, and Y. J. Chabal, *J. Am. Chem. Soc.* **134**, 15201 (2012).
  - <sup>5</sup> K. Lee, J. D. Howe, L.-C. Lin, B. Smit, and J. B. Neaton, *Chem. Mater.* **27**, 668 (2015).
  - <sup>6</sup> J. Y. Lee, O. Farha, J. Roberts, K. A. Scheidt, S. T. Nguyen, and J. T. Hupp, *Chem. Soc. Rev.* **38**, 1450 (2009).
  - <sup>7</sup> I. Luz, F. X. Llabrés i Xamena, and A. Corma, *J. Catal.* **276**, 134 (2010).
  - <sup>8</sup> T. Uemura, N. Yanai, and S. Kitagawa, *Chem. Soc. Rev.* **38**, 1228 (2009).
  - <sup>9</sup> M. J. Vitorino, T. Devic, M. Tromp, G. Férey, and M. Visseaux, *Macromol. Chem. Phys.* **210**, 1923 (2009).
  - <sup>10</sup> M. D. Allendorf, C. A. Bauer, R. K. Bhakta, and R. Houk, *Chem. Soc. Rev.* **38**, 1330 (2009).
  - <sup>11</sup> K. A. White, D. A. Chengelis, K. A. Gogick, J. Stehman, N. L. Rosi, and S. Petoud, *J. Am. Chem. Soc.* **131**, 18069 (2009).
  - <sup>12</sup> S. Bordiga, C. Lamberti, G. Ricchiardi, L. Regli, F. Bonino, A. Damin, K.-P. Lillerud, M. Bjorgen, and A. Zecchina, *Chem. Commun.*, 2300 (2004).
  - <sup>13</sup> M. Kurmoo, *Chem. Soc. Rev.* **38**, 1353 (2009).
  - <sup>14</sup> P. Horcajada, T. Chalati, C. Serre, B. Gillet, C. Sebrie, T. Baati, J. Eubank, D. Heurtaux, P. Clayette, C. Kreuz, J.-S. Chang, Y. Hwang, V. Marsaud, P.-N. Bories, L. Cynober, S. Gil, G. Férey, P. Couvreur, and R. Gref, *Nat. Mater.* **9**, 172 (2010).
  - <sup>15</sup> A. Stroppa, P. Jain, P. Barone, M. Marsman, J. M. Perez-Mato, A. K. Cheetham, H. W. Kroto, and S. Picozzi, *Angew. Chem., Int. Ed.* **50**, 5847 (2011).
  - <sup>16</sup> A. Stroppa, P. Barone, P. Jain, J. M. Perez-Mato, and S. Picozzi, *Adv. Mater.* **25**, 2284 (2013).
  - <sup>17</sup> D. Di Sante, A. Stroppa, P. Jain, and S. Picozzi, *J. Am. Chem. Soc.* **135**, 18126 (2013).
  - <sup>18</sup> C. Serre, C. Mellot-Draznieks, S. Surblé, N. Audebrand, Y. Filinchuck, and G. Férey, *Science* **315**, 1828 (2007).
  - <sup>19</sup> M. D. Allendorf, R. J. T. Houk, L. Andruskiewicz, A. A. Talin, J. Pikarsky, A. Choudhury, K. A. Gall, and P. J. Henske, *J. Am. Chem. Soc.* **130**, 14404 (2008).
  - <sup>20</sup> J.-C. Tan and A. K. Cheetham, *Chem. Soc. Rev.* **40**, 1059 (2011).
  - <sup>21</sup> L. Kreno, K. Leong, O. Farha, M. Allendorf, R. Van Duyne, and J. Hupp, *Chem. Rev.* **112**, 1105 (2012).
  - <sup>22</sup> P. Canepa, K. Tan, Y. Du, H. Lu, Y. J. Chabal, and T. Thonhauser, *J. Mater. Chem. A* **3**, 986 (2015).
  - <sup>23</sup> P. M. Schoenecker, C. G. Carson, H. Jasuja, C. J. J. Fleming, and K. S. Walton, *Ind. Eng. Chem. Res.* **51**, 6513 (2012).
  - <sup>24</sup> J. B. DeCoste, G. W. Peterson, B. J. Schindler, K. L. Killops, M. A. Browe, and J. J. Mahle, *J. Mater. Chem. A* **1**, 11922 (2013).
  - <sup>25</sup> A. C. Kizzie, A. G. Wong-Foy, and A. J. Matzger, *Langmuir* **27**, 6368 (2011).
  - <sup>26</sup> T. Remy, S. A. Peter, S. Van der Perre, P. Valvekens, D. E. De Vos, G. V. Baron, and J. F. M. Denayer, *J. Phys. Chem. C* **117**, 9301 (2013).
  - <sup>27</sup> J. Liu, A. I. Benin, A. M. B. Furtado, P. Jakubczak, R. R. Willis, and M. D. LeVan, *Langmuir* **27**, 11451 (2011).
  - <sup>28</sup> K. Tan, S. Zuluaga, Q. Gong, P. Canepa, H. Wang, J. Li, Y. J. Chabal, and T. Thonhauser, *Chem. Mater.* **26**, 6886 (2014).
  - <sup>29</sup> K. Tan, N. Nijem, Y. Gao, S. Zuluaga, J. Li, T. Thonhauser, and Y. J. Chabal, *CrystEngComm* **17**, 247 (2015).
  - <sup>30</sup> S. S. Han, S.-H. Choi, and A. C. T. van Duin, *Chem. Commun.* **46**, 5713 (2010).
  - <sup>31</sup> S. Zuluaga, E. M.-A. Fuentes-Fernandez, K. Tan, F. Xu, J. Li, Y. J. Chabal, and T. Thonhauser, *J. Mater. Chem. A* **4**, 5176 (2016).
  - <sup>32</sup> K. Tan, S. Zuluaga, Q. Gong, Y. Gao, N. Nijem, J. Li, T. Thonhauser, and Y. J. Chabal, *Chem. Mater.* **27**, 2203 (2015).
  - <sup>33</sup> P. Canepa, C. A. Arter, E. M. Conwill, D. H. Johnson, B. A. Shoemaker, K. Z. Soliman, and T. Thonhauser, *J. Mater. Chem. A* **1**, 13597 (2013).
  - <sup>34</sup> J. Carrasco, A. Hodgson, and A. Michaelides, *Nat. Mater.* **11**, 667 (2012).
  - <sup>35</sup> S. Maheshwary, N. Patel, N. Sathyamurthy, A. D. Kulkarni, and S. R. Gadre, *J. Phys. Chem. A* **105**, 10525 (2001).
  - <sup>36</sup> S. Nie, P. J. Feibelman, N. C. Bartelt, and K. Thürmer, *Phys. Rev. Lett.* **105**, 026102 (2010).
  - <sup>37</sup> P. J. Feibelman, N. C. Bartelt, S. Nie, and K. Thürmer, *J. Chem. Phys.* **133**, 154703 (2010).
  - <sup>38</sup> M. A. Henderson, *Surf. Sci. Rep.* **46**, 1 (2002).
  - <sup>39</sup> B. Kolb and T. Thonhauser, *Phys. Rev. B* **84**, 045116 (2011).
  - <sup>40</sup> B. Meyer, D. Marx, O. Dulub, U. Diebold, M. Kunat, D. Langenberg, and C. Wöll, *Angew. Chemie Int. Ed.* **43**, 6641 (2004).
  - <sup>41</sup> G. Tocci and A. Michaelides, *Phys. Chem. Lett.* **5**, 474 (2014).
  - <sup>42</sup> K. C. Hass, W. F. Schneider, A. Curioni, and W. Andreoni, *Science* **282**, 265 (1998).
  - <sup>43</sup> L. Giordano, J. Goniakowski, and J. Suzanne, *Phys. Rev. Lett.* **81**, 1271 (1998).
  - <sup>44</sup> M. Odelius, *Phys. Rev. Lett.* **82**, 3919 (1999).
  - <sup>45</sup> Y. Lei, Z. X. Guo, W. Zhu, S. Meng, and Z. Zhang, *Appl. Phys. Lett.* **91**, 161906 (2007).
  - <sup>46</sup> M. K. Kostov, E. E. Santiso, A. M. George, K. E. Gubbins, and M. B. Nardelli, *Phys. Rev. Lett.* **95**, 136105 (2005).
  - <sup>47</sup> A. Tilocca and A. Selloni, *J. Chem. Phys.* **119**, 7445 (2003).
  - <sup>48</sup> M. Miao, Y. Liu, Q. Wang, T. Wu, L. Huang, K. E. Gubbins, and M. B. Nardelli, *J. Chem. Phys.* **136**, 064703 (2012).

- (2012).
- <sup>49</sup> P. Giannozzi, S. Baroni, N. Bonini, M. Calandra, R. Car, C. Cavazzoni, D. Ceresoli, G. L. Chiarotti, M. Cococcioni, I. Dabo, A. Dal Corso, S. de Gironcoli, S. Fabris, G. Fratesi, R. Gebauer, U. Gerstmann, C. Gougousis, A. Kokalj, M. Lazzeri, L. Martin-Samos, N. Marzari, F. Mauri, R. Mazzarello, S. Paolini, A. Pasquarello, L. Paulatto, C. Sbraccia, S. Scandolo, G. Sclauzero, A. P. Seitsonen, A. Smogunov, P. Umari, and R. M. Wentzcovitch, *J. Phys. Condens. Matter* **21**, 395502 (2009).
- <sup>50</sup> T. Thonhauser, S. Zuluaga, C. A. Arter, K. Berland, E. Schröder, and P. Hyldgaard, *Phys. Rev. Lett.* **115**, 136402 (2015).
- <sup>51</sup> K. Berland, V. R. Cooper, K. Lee, E. Schröder, T. Thonhauser, P. Hyldgaard, and B. I. Lundqvist, *Reports Prog. Phys.* **78**, 066501 (2015).
- <sup>52</sup> D. C. Langreth, B. I. Lundqvist, S. D. Chakarova-Käck, V. R. Cooper, M. Dion, P. Hyldgaard, A. Kelkkanen, J. Kleis, L. Kong, S. Li, P. G. Moses, E. D. Murray, A. Puzder, H. Rydberg, E. Schröder, and T. Thonhauser, *J. Phys. Condens. Matter* **21**, 084203 (2009).
- <sup>53</sup> T. Thonhauser, V. R. Cooper, S. Li, A. Puzder, P. Hyldgaard, and D. C. Langreth, *Phys. Rev. B* **76**, 125112 (2007).
- <sup>54</sup> J. M. McMahon, M. A. Morales, B. Kolb, and T. Thonhauser, arXiv: 1402.2697 (2014).
- <sup>55</sup> G. Henkelman, B. P. Uberuaga, and H. Jónsson, *J. Chem. Phys.* **113**, 9901 (2000).
- <sup>56</sup> G. Henkelman and H. Jónsson, *J. Chem. Phys.* **113**, 9978 (2000).
- <sup>57</sup> W. Zhou, H. Wu, and T. Yildirim, *J. Am. Chem. Soc.* **130**, 15268 (2008).